

Multifunctional Oxygenated Particles for Targeted Cancer Drug Delivery and Evaluation with Darkfield Hyperspectral Imaging

Yi Wen, Wenjie Liu, Benjamin David, Wen Ren, and Joseph Irudayaraj*

Cite This: *ACS Omega* 2022, 7, 41275–41283

Read Online

ACCESS |



Metrics & More

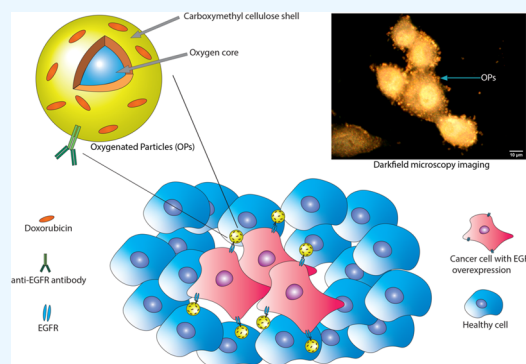


Article Recommendations



Supporting Information

ABSTRACT: We propose a novel multifunctional nanocarrier system for targeted drug delivery for lung cancer theranostics. Oxygenated particles (OPs) synthesized with an oxygen-encapsulating carboxymethyl cellulose shell were used as a platform to deliver oxygen to the hypoxic tumor microenvironment. The OPs synthesized could also be conjugated with ligands (e.g., antibodies) to target cancer cells expressing the corresponding antigens to deliver a drug, doxorubicin. In vitro testing of functionalized OPs showed increased efficacy of doxorubicin against the proliferation of lung cancer cells. Both confocal fluorescence imaging and darkfield microscopy hyperspectral imaging validated the OP complex and its efficient targeting of specific cells to deliver the therapeutic. The nanocarrier platform developed can also serve as a diagnostic imaging reagent as demonstrated by darkfield microscopy. Results show that the theranostic OPs developed with multifunctional modalities enabled targeted drug delivery with improved efficacy and tracking of drug delivery vehicles by imaging.



INTRODUCTION

An estimated 236,740 new cases of lung cancer will be diagnosed and 130,180 deaths will occur in 2022 in the United States. Lung cancer is one of the most common causes of cancer deaths among both sexes, amounting to a quarter of all cancer deaths.¹ Late diagnoses and limited treatment options are cited as major causes for the high mortality rate of lung cancer patients.² Of all lung cancer cases, around 84% are non-small-cell lung cancer,¹ which was resistant to treatment due to its complex pathological mechanisms.³ Cancer cells express several protein biomarkers as cell surface receptors. Epidermal growth factor receptor (EGFR) is a transmembrane receptor tyrosine kinase that is expressed in many normal epithelial, neurogenic, and mesenchymal tissues. Previous studies have implicated a positive correlation between EGFR overexpression or mutation and poor prognosis.^{3,4} Thus, EGFR can be used as a surface marker for cancer diagnosis or for targeted drug delivery to treat lung cancer. EGFR inhibitors have been used to target and treat EGFR overexpressing cancer cells with promising treatment outcomes in some patients.⁵

Due to both short-term and long-term adverse effects of chemotherapy agents, which sometimes can be lethal, dosage sufficient to treat certain cancers often cannot be administered.⁶ The efficiency of free chemotherapeutic drugs can be low due to free dispersal throughout the body. For instance, cisplatin can be taken up and accumulated in the liver and kidney, causing severe hepatotoxicity and nephrotoxicity.⁷ Doxorubicin is a widely used chemotherapeutic agent, which is an antibiotic derived from bacterium *Streptomyces peucetius*. The drug functions by intercalating DNA base pairs to cause

DNA strand breakage. However, it has potentially lethal adverse effects, especially in cardiac tissues.⁸ Doxorubicin has emerged as a good model drug to test the delivery system due to its pharmacological and diagnostic functionality enabled by its intrinsic fluorescence.^{9,10} Targeted delivery is a highly desired attribute because it has the potential to decrease drug toxicity in healthy tissues while targeting the diseased with higher efficiency. Nanoparticles (NPs) have been used as carriers to deliver chemotherapeutic drugs via biochemical or physical mechanisms as a viable form of therapeutics delivery.^{11–13} NPs can also be developed to co-deliver different combinations of drugs while increasing the efficacy and minimizing the side effects of each of these drugs.⁵ Nanocarrier systems can also deliver pro-drugs, so that an active drug is only formed at the location of interest.¹⁴ Some nanocarrier systems can also perform on-demand drug release, in response to a mechanical or chemical trigger.^{15,16} NPs have been designed to confer multimodal or multi-functional attributes ranging from drug delivery to diagnosis and imaging.^{17–20} With the cancer targeting functionality, these nanocarriers can also be used to target cancerous tissues for diagnostic purposes.

Received: August 4, 2022

Accepted: October 20, 2022

Published: November 1, 2022



Hypoxia is a common condition in tumor tissues and hypoxia-driven pathways can exacerbate tumor growth.^{21,22} In our previous works, we demonstrated that the oxygen-encapsulated carboxymethyl cellulose (CMC) shell can be triggered to release oxygen in a hypoxic and acidic environment around and inside tumor cells.²³ CMC is an FDA-approved pharmaceutical excipient. CMC-based oxygen nanobubbles possess a unique refractive index at the oxygen/shell interface and can be imaged with a hyperspectral dark-field microscope.²⁴ However, our previous efforts in oxygen nanobubble research were primarily systemic in nature and did not target specific cells of interest. In this work, we demonstrate an oxygen-encapsulated multifunctional nanocarrier system for targeted drug delivery and hypoxia mitigation.

Traditionally, fluorescence microscopy imaging has been used to evaluate the interaction between targeted nanocarriers and cells or tissues; therefore, diagnosing cancer tissues with high specificity is possible. Herein, labeling nanoparticles with fluorophores is a primary requirement. Primary antibodies tagged with fluorophores are not only costly but can also limit both the synthesis and functional properties of the nanoparticle system due to their binding efficacy and spatial occupation. Another unique attribute of our nanocarrier system is to circumvent the labeling for imaging by fluorescence microscopy with darkfield microscopy (DFM), which can be label-free. DFM coupled with a hyperspectral imaging system (HSI) can be used to identify many nanoparticles with their "signature" spectrum.^{25,26} DFM–HSI can achieve high signal-to-noise ratio and can record high-resolution spectrum at every pixel of the image. A DFM–HSI system is also particularly suitable for imaging single cells to characterize subcellular structures in both live and fixed cells.^{27,28}

We propose the development of multifunctional oxygenated particles (OPs) for both doxorubicin-targeted delivery and mitigation of hypoxia to improve drug efficacy and human non-small-cell lung carcinoma cell diagnosis. We evaluated antibody-modified and drug-loaded OPs for effective targeting of cancer cell surface receptors for the targeted drug delivery and imaging. The size of the OPs is tunable with the proposed protocol in the range from 0.2 to 2 μm . The multifunctional OPs were characterized with confocal fluorescence microscopy and dark-field imaging. In this study, particles within sub-micron to micrometer size range (0.5–2 μm) were used because they could be imaged with higher visual clarity.

MATERIALS AND METHODS

OP Synthesis. OPs were synthesized via a cross-linking reaction of the CMC monomers. First, 0.1–1% (w/v) sodium carboxymethyl cellulose was thoroughly dispersed in Milli-Q water by mixing with a homogenizer (Ultra-TURRAX T18, IKA; Wilmington, NC, USA) at 5600 rpm for 3 min. Then, the homogenization revolving speed was reduced to 2800 rpm and continued till the end of synthesis. The solution was oxygenated for 15 min to saturate the solution with oxygen. While 1–2% v/v FC-72 (AC123791000, Fisher Scientific, Hanover Park, IL, USA) was added to the solution to increase the oxygen solubility in solution. During oxygenation, the solution was sonicated with a probe sonicator (Branson Sonifier SFX250, Emerson; St. Louis, MO, USA) with a microtip continuously at 55% power output to speed up the gas exchange. 0.005–0.01% v/v TWEEN 20 (P9416, Sigma-Aldrich, St. Louis, MO, USA) was added immediately after

oxygenation. Then, the sonication was changed to the pulsing mode with 0.2 s interval at 70% power output to compress and produce nano- and micro-sized OPs.²⁹ During a period of 120 s, 0.2–0.5% v/v of a 0.1–1% w/v aluminum chloride solution was added to cross-link the CMC monomers around the nano/micro-OPs to form oxygen-encapsulated particles with the CMC shell. Then, 0.5% ammonium hydroxide solution was added dropwise to neutralize. Particles of different sizes obtained in the final solution were separated by centrifugation or ultracentrifugation. Separated particles are dissolved and stored in sterilized water. All experiments were performed with particles made within 30 days.

Antibody Conjugation. Conjugation of antibodies onto OPs were performed via EDC (1-ethyl-3-(3-dimethylaminopropyl)carbodiimide hydrochloride) (22980, Fisher Scientific, Hanover Park, IL, USA) mediated reaction. Protocol was modified per manufacturer's instruction. OPs were centrifuged to remove the liquid medium used to suspend the particles. Particles were redispersed in 10 mM MES buffer (pH = 4.7). Freshly prepared 20% v/v 100 mM EDC in water was immediately added to the particle solution, along with anti-EGFR antibodies (PIMA513269, Fisher Scientific) proportional to the OPs. The reaction was carried out in a microcentrifuge tube and rotated on a rotator for 6 h. Then, the solution was spun down to remove the unreacted EDCs and antibodies. The pellet was washed twice with MES buffer following short centrifugation. Pellets were then redispersed in water for doxorubicin loading.

Doxorubicin Loading. 5% v/v of 0.2 mg/mL doxorubicin (Sigma-Aldrich, St. Louis, MO, USA) was added to the antibody-conjugated OPs. The mixture was spun on a rotator for 10 min to achieve maximum loading. Then, the solution was spun down to remove the unreacted doxorubicin. Pellets were then washed with Milli-Q water following short centrifugation. Finally, doxorubicin-loaded and antibody-conjugated OPs were dissolved in PBS and stored at 4 °C.

Cell Culture. Human non-small cell lung carcinoma cell line A549 (ATCC; Manassas, VA, USA) was used as an *in vitro* model to evaluate targeted drug delivery with anti-EGFR antibody-conjugated OP conjugates. Epidermal growth factor receptor (EGFR/HER1) was identified as a prominent marker of the lung cancer cells and EGFR was chosen as the target because it is highly expressed in A549 cells³⁰ (Figure 2H).

A549 cells were cultured in the culture medium of 89% Ham's F-12K Medium (Gibco, Fisher Scientific), 10% v/v fetal bovine serum (Gibco, Fisher Scientific), and 1% w/w penicillin streptomycin Solution (Corning; Corning, NY, USA). Cells were cultured in a humidified incubator with 5% carbon dioxide at 37 °C. Cells were fixed with 4% paraformaldehyde (Sigma-Aldrich, St. Louis, MO, USA) in PBS prior to experimentation with OP.

WST-1 Cell Proliferation Assay. The WST-1 assay was performed on lung carcinoma cells following different treatments to assess their impact on cancer cell proliferation. Around 7500 A549 cells were passaged in a 96-well plate and grown for 24 h to achieve 30–40% confluency, following the corresponding treatments. Cytotoxicity of doxorubicin was tested for concentrations of 0.1, 0.5, 1, 2, or 5 μM to determine the level of doxorubicin that exerts an effective but non-lethal cytotoxic effect on A549 cells (Figure 3C). Finally, a concentration of 0.5 μM was chosen from the tested conditions and added to the doxorubicin-only (DOX) treatment group. Figure 3D shows the cell proliferation results

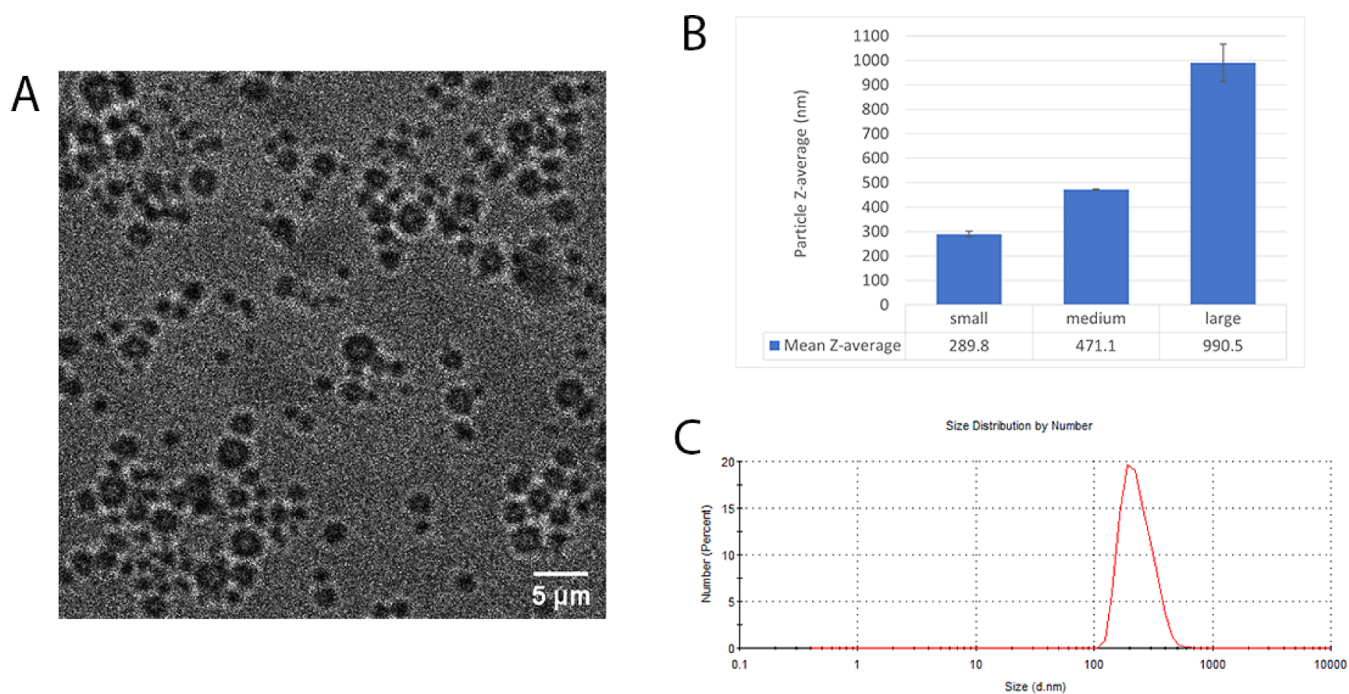


Figure 1. Characterization of OPs. (A) Confocal brightfield image of OP with different sizes. (B) Three different sizes of OP obtained from separation method. (C) Example size distribution of ONBs with Z-average of 289.8 nm, taken with DLS.

after 48 h of treatment. For the negative control, media was added to the control. Anti-EGFR antibody-conjugated doxorubicin-loaded OPs were added to cells to attain a concentration of 0.5 μM doxorubicin in the antiEGFR-DOX-OP group. OPs or anti-EGFR antibody-conjugated OPs with an equivalent amount of OP to the experimental group were added to their corresponding groups.

Cell proliferation reagent WST-1 (Roche, Pleasanton, CA, USA) was added into the media after 48 h of treatment. After 30 min of incubation at 37 $^{\circ}\text{C}$, absorbance of the formazan product at 440 nm wavelength was measured with a reference reading obtained at 600 nm wavelength.

OP Characterization. The size distribution of the synthesized OPs with different size profiles was measured with dynamic light scattering (DLS) using a Zetasizer Nano ZS (Malvern Instruments; Worcestershire, UK). Data was analyzed with Zetasizer software.

The amount of doxorubicin loaded onto OPs was assessed with a microplate reader. The doxorubicin fluorescence signal was excited at 485 nm; and emission measured at 590 nm wavelength. To assess whether OPs interfere with the fluorescence signal from doxorubicin, concentrated OPs were added to 1 or 10 μM DOX. The doxorubicin fluorescence signal with or without the presence on nanoparticles was measured and presented in Figure 3A. To show that doxorubicin fluorescence is linearly correlated to its concentration between 0 and 20 μM , a standard curve was developed (Figure 3B).

Confocal Fluorescence Microscopy. Confocal fluorescence microscopy (CFM) was used to confirm both the successful conjugation of antibodies onto OPs and the loading of doxorubicin. CFM was also utilized to validate the specificity of the anti-EGFR antibody targeting the EGFR receptors on A549 cells, as well as the biomolecular or cellular targeting of antibody-conjugated OPs. Goat anti-mouse IgG secondary

antibody with Alexa Fluor 488 (A-11001, Fisher Scientific) and a mouse IgG (Fisher Scientific) were used.

Confocal fluorescence images were obtained with an Alba Confocal Fluorescence Lifetime Imaging system (ISS, Champaign, USA). Details of the system are as described previously.³¹ Briefly, a 488 nm picosecond pulsed laser at 50 MHz repetition rate was used as the excitation source, and the emission passed through an apochromatic water immersion objective (60 \times , NA = 1.2, Olympus). Photons were collected by the same objective, then passed through a 50 mm pinhole, and a 525/50 (for Alexa488) and 593/40 (for doxorubicin) emission filter (Chroma) before reaching an avalanche photodiode (SPCM-AQRH-15, Excelitas).

Darkfield Microscopy and Hyperspectral Imaging. Darkfield microscopy was used to image OPs and its interaction with cells. Images were first obtained with an AmScope camera (Irvine, CA, USA). Hyperspectral images were acquired with a CytoViva hyperspectral camera (Autum, AL, USA) and processed with CytoViva version of ENVI 4.8 software (Exelis Visual Information Solutions; Boulder, CO, USA). Images were also analyzed with ImageJ software (64 bit Java 1.8.0_112, NIH, Bethesda, Maryland, USA). Detailed image processing details were adapted from our previous work and described in the Supporting Information and Figure S3.³²

Statistics. For comparison of the DOX fluorescence signal with or without OPs, three replicates were used, and an unpaired *t*-test was performed. For cytotoxicity assessment from different treatments levels, six sets of independent biological replicates of each treatment group were performed. Average values of technical replicates were used to eliminate the noise from instrumentation and measurements. Within each set, the data of experimental groups were normalized to the control group. Normality was tested within each treatment group with the Shapiro–Wilk test. Unpaired *t*-test was performed for this case–control study.

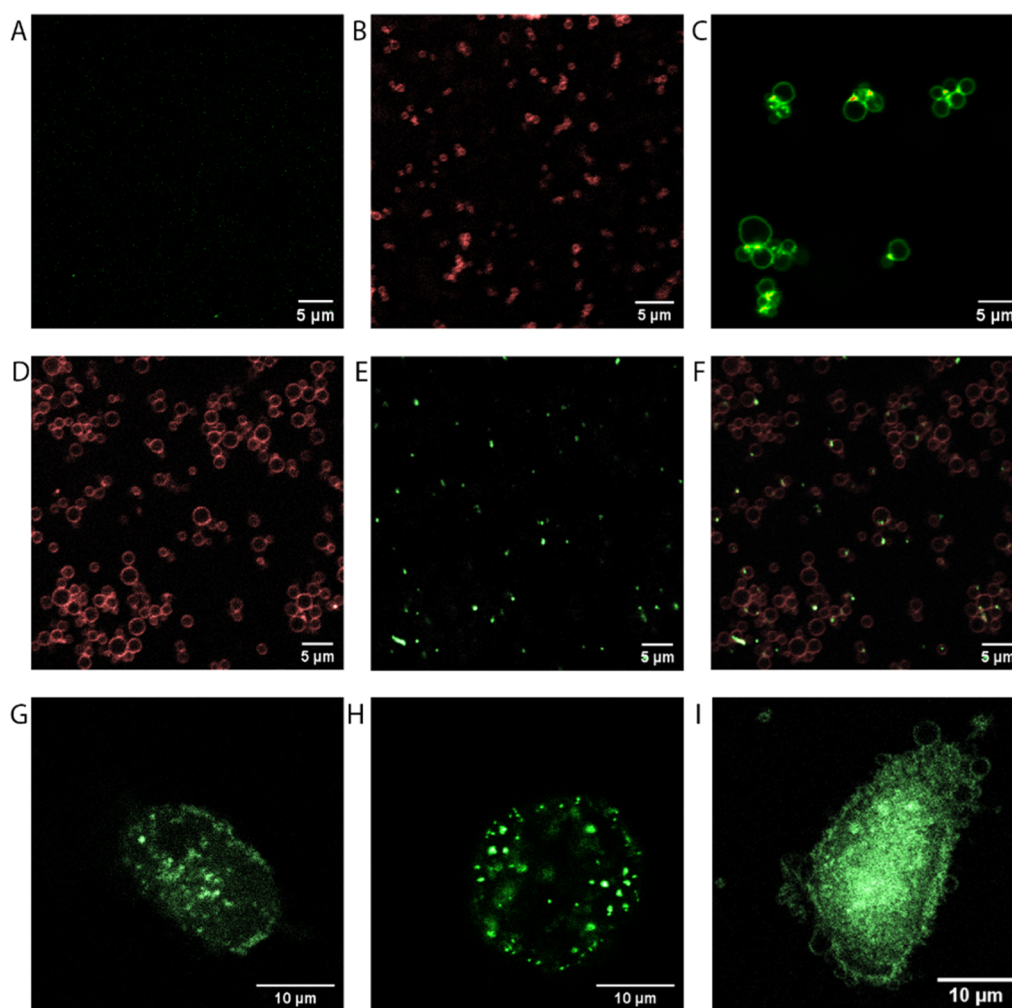


Figure 2. Confocal fluorescence microscopy imaging of functionalized OPs and its interaction with A549 cells. (A) OPs with primary antibody do not have an intrinsic fluorescence signal. (B) OPs loaded with doxorubicin. (C) Functionalized OPs that can target free protein molecule. (D) Doxorubicin fluorescence signal on functionalized oxygenated micro-particles. (E) Functionalized oxygenated micro-particles incubated with secondary antibody with fluorophore to locate conjugated primary antibody. (F) Overlaid image of (D,E). (G) Intrinsic autofluorescence of A549 cell. (H) Anti-EGFR antibody-specific interaction with A549 cell. (I) Functionalized OP complex specific interaction with A549 cell.

RESULTS AND DISCUSSION

OP Characterization. The synthesized OPs consist of a gaseous oxygen core encapsulated by a layer of polymeric cellulosic shell. Brightfield images of a mixture of OPs are shown in Figure 1A. Nonuniformity of the refractive index due to the core–shell structure generates light scattering conducive to DFM–HSI imaging.^{24,33} The synthesis parameters can be adjusted to formulate both nano-sized and micro-sized particles. Post-synthesis separation via centrifugation and ultracentrifugation can be used to obtain monodispersed OPs with the desired size. Particle size diameter was measured with DLS. Figure 1C shows the dispersion of OPs with an average diameter of 300 nm. Figure 1B shows small, medium, and large OPs that were separated by 15,000 rpm, 10,000 rpm, or 4000 rpm centrifugation, respectively. With DFM–HSI, OPs less than 500 nm in diameter that could contribute to higher light scattering was used for dark-field imaging purposes. For confocal imaging, particles in the micro to sub-micron range were used in our experiments, due to their clear optical resolution that helped us to identify and demonstrate the interaction between particles and cells. Although the particle size can be varied as shown in this work, particles larger than

200 nm in diameter can more easily be cleared from the circulatory system into the liver or kidney.³⁴ Oxygen inside the particles can be released when placed in an acidic environment induced by the breakage of the particles and acts as a supplement to treat hypoxic conditions in tumors, as shown in our previous studies.^{23,35} OP complexes conjugated with antibodies loaded with doxorubicin were imaged with both confocal brightfield microscopy fluorescence imaging (Figure 2D–F) and darkfield microscopy hyperspectral imaging (Figures 4A and 5A).

Antibody Conjugation Validation. Anti-EGFR antibody was selected because EGFR are widely and highly expressed in lung cancer cells.⁴ Previous studies have shown the uptake of EGF-conjugated nanoparticles mediated by EGFR in A549 cells.³⁶ Having OPs conjugated with the anti-EGFR antibody will facilitate the targeted delivery of molecular cargos to cancer cells. Blocking the EGFR on cancer cells can also impair cancer cellular activities through the inhibition mechanism.³⁷ EDC-mediated conjugation between anti-EGFR antibody and CMC shell was performed because the antibody comprises amine groups and CMC particles contained carboxyl groups (Figure S1). Because the anti-EGFR antibodies were of mouse

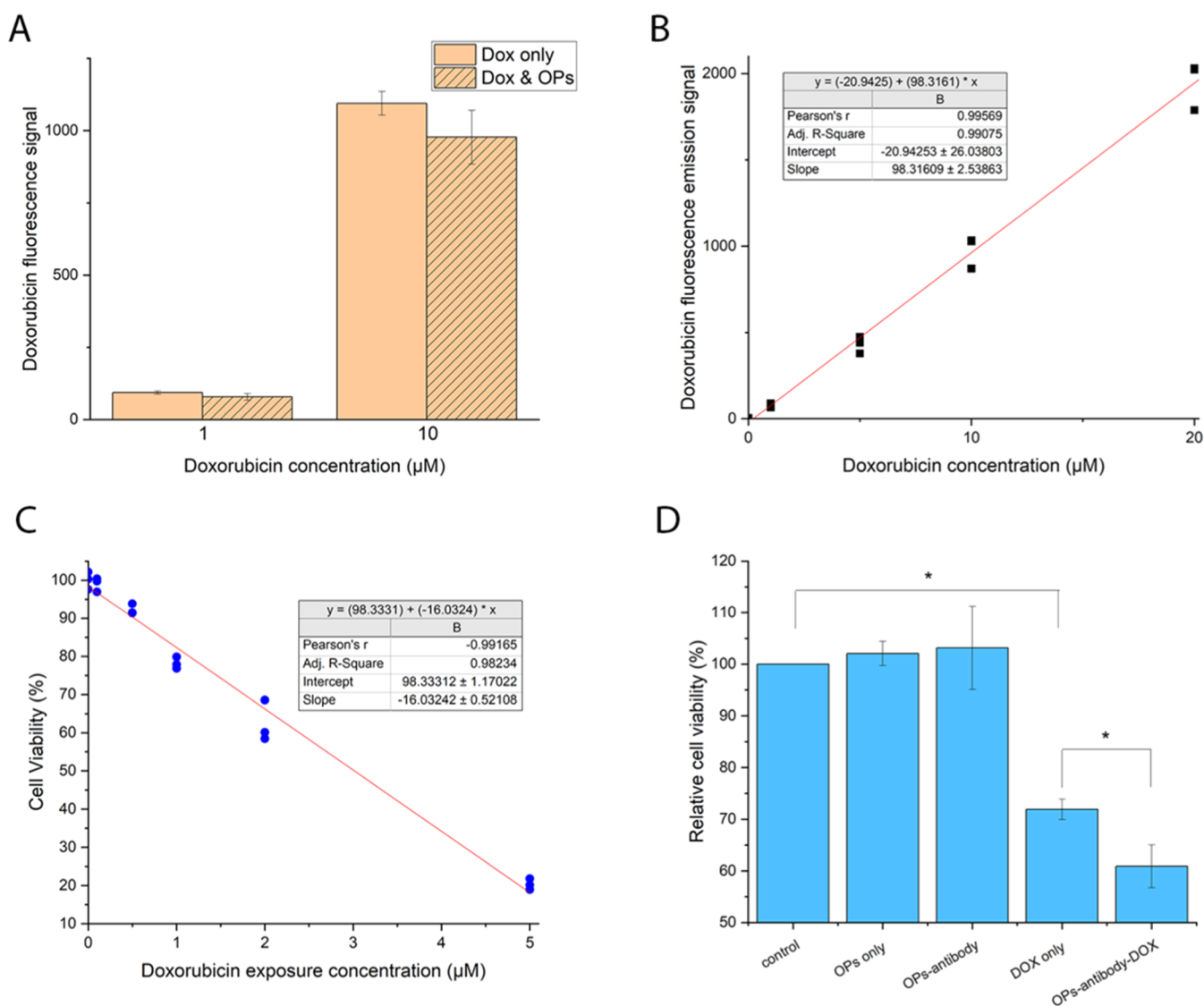


Figure 3. Targeted drug delivery with antibody-conjugated OP showing increased treatment efficacy. (A) Fluorescence signal of doxorubicin with or without OPs mixed in the solution; error bar represents standard deviation, $n = 3$. (B) Calibration curve to correlate the doxorubicin concentrations with fluorescence signals. (C) Cytotoxicity of doxorubicin on A549 cells through the WST-1 assay. (D) A549 cell proliferation assay with different treatments; error bar represents standard error of mean, $n = 6$; * p -value < 0.05.

origin, the successful conjugation was accomplished by using a secondary anti-mouse antibody labeled with fluorophore (Alexa488). Signals of the secondary antibodies conjugated to the primary antibody on OPs can be seen in Figure 2E, and this figure was merged with doxorubicin fluorescence signals (Figure 2F) to show the localization on OPs.

Doxorubicin Loading Validation. Doxorubicin was selected as a model drug because of its intrinsic fluorescence and wide usage in the treatment of lung cancer.⁸ OPs conjugated with only anti-EGFR antibody were imaged and did not contribute to any fluorescence, as expected (Figure 2A). The fluorescence signal from the particles was evident upon successful loading of doxorubicin onto the CMC shell of both submicron sized (Figure 2B) and micrometer sized OPs (Figure 2D). Figure 2B further shows that OPs with doxorubicin had a shelf life of at least 30 days in a neutral pH environment at 4 °C. Carboxyl groups on the polymerized CMC chains (Figure S1) can be negatively charged at neutral pH, while solvated doxorubicin has an amine group that is

positively charged at neutral pH because the pK_a of a primary amine group is larger than 7.0.³⁸ $pK_a = 8.46$ for the amine group on doxorubicin.³⁹ We expect doxorubicin to be conjugated to the surface of the CMC shell due to the electrostatic interaction. Utilizing the same concept, CMC OPs were loaded with two other chemicals with positively charged functional groups, rhodamine 6G (989-38-8, Sigma-Aldrich, St. Louis, MO, USA) and Dil dye (D3911, Fisher Scientific, Hanover Park, IL, USA) (Figure S2). Instead of forming a covalent bond between doxorubicin and the CMC shell or encapsulate doxorubicin inside of the delivery vessel, the mechanism of electrostatic interaction was found to be more suitable for drug release studies in tumor tissues. Without the need to disintegrate the CMC shell, oxygen can be released for a prolonged period to mitigate the hypoxic tumor micro-environment. On the other hand, an acidic tumor micro-environment can trigger the separation of doxorubicin from the CMC shell.

To quantify doxorubicin loading onto OPs, fluorescence was measured for 1 or 10 μM concentration of doxorubicin with or without the addition of concentrated OPs. We did not observe any statistically significant difference in either case (Figure 3A, 1 μM p -value = 0.1153, 10 μM p -value = 0.1163). Therefore, a standard curve of DOX with OPs was developed to correlate the fluorescence levels from doxorubicin with the corresponding concentrations. As shown in Figure 3B, a linear relationship was obtained between 0 and 20 μM of doxorubicin (Adj. R^2 = 0.9907). From this linear standard curve, we note that doxorubicin loading in functionalized OPs could be in the range between 5 and 10 μM .

Drug Delivery through OPs Increased the Efficacy of Doxorubicin. A cytotoxicity assay of doxorubicin on A549 cells was performed with the WST-1 assay. A linear relationship was noted between cell proliferation rates and doxorubicin treatment concentrations between 0 and 5 μM (Figure 3C, R^2 = 0.9834). With these results, 0.5 μM doxorubicin was chosen for the following studies due to its small but significant impact on A549 cells.

Because increased cell proliferation is one of the most profound features of cancer cells, WST-1 proliferation assay was used to assess the efficacy of doxorubicin and its equivalent dosage delivered with functionalized CMC OPs. For nine sets of biological replicates, each experimental group was compared with its corresponding control group. No significant difference was noted between the control and cells treated with unmodified OPs (p -value is 0.1038) or between the control and cells treated with OP complexes conjugated with anti-EGFR antibodies (p -value is 0.5526). A 26.06% decrease in proliferation was noted 48 h after 0.5 μM doxorubicin treatment. In contrast, a 39.08% decrease in proliferation was noted in the groups treated with 0.5 μM doxorubicin delivered with anti-EGFR antibody-conjugated OPs. More importantly, a significant increase of up to 39.19% in the inhibition potential of cancer cell proliferation was achieved with doxorubicin administration using the OP delivery platform (p -value is 0.0372) relative to doxorubicin treatment alone. Thus, assisted with a targeting ligand, delivery of cargo with functionalized OPs can increase drug efficacy significantly. Based on our previous studies, oxygen released from nanoparticles has the potential to revert hypoxia by methylation programming and alter the expression of hypoxia-related factors.²³ However, in this study, we hypothesize that oxygen can act as a chemotherapy drug sensitizer, as in our prior study.³³ We note from Figure 3D that without doxorubicin, OPs or antibody-conjugated OPs alone were not able to decrease the viability of A549 cells.

Fluorescence Imaging of Functionalized OP Targeting Lung Cancer Cells. First, our functionalized OP complexes were tested to target free protein molecules. Besides cells, our OPs were found to target single biomolecules such as hormones. In this case, the anti-mouse antibody labeled with Alexa Fluor 488 was conjugated onto the surface of OPs. Free mouse IgG was used as a model targeting ligand in our OP system to validate target binding. Confocal fluorescence microscopy (CFM) images shown in Figure 2C indicate that multiple functionalized OPs could bind to the model system. Our previous work has shown the targeting of EGFR in live cells with fluorescence correlation spectroscopy.¹⁹ Human non-small cell lung carcinoma cell line A549 was chosen as the model system to demonstrate our target binding study and evaluated with both CFM and DFM–HSI.

Using CFM, the autofluorescence of A549 was shown to be minimal (Figure 2G). To test the specificity of anti-EGFR antibody on A549 cells, fixed A549 cells were incubated with diluted anti-EGFR antibodies for an hour. Cells were then washed thoroughly and incubated with secondary antibody with Alexa Fluor 488 for 1 h with another wash. Figure 2H shows that EGFR was expressed throughout the surface of A549 cell. Our functionalized OP complexes were then tested by incubating with A549 cells in the same fashion as with free antibody. Due to the intrinsic fluorescence of doxorubicin, the functionalized OP complexes could be visualized and their targeting of A549 cells was evident (Figure 2I).

Hyperspectral Imaging of the Functionalized OPs Targeting Lung Cancer Cells. Dark-field microscopy (DFM) was used either for standalone detection or in combination with hyperspectral imaging (HSI) to further demonstrate that our OP complexes could successfully target cancer cells. Figure 4C shows the presence of OP complexes

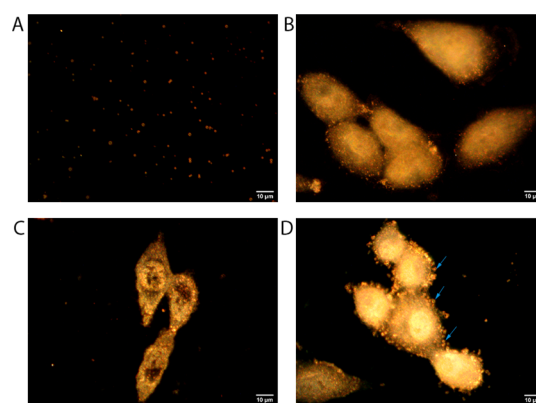


Figure 4. Darkfield microscopy images of OPs and cells. (A) OP complex. (B) A549 cells only. (C) A549 cells after incubation with OPs without modifications. (D) A549 cells after incubation with the functionalized OP complex.

under DFM with a regular camera for better resolution and visualization. A549 cells without modification were shown in Figure 4B as a control image. After incubation with OPs without antibody conjugation, A549 cells did not retain any OP (Figure 4C). Finally, A549 cells with functionalized OP complexes bound after incubation was also shown (Figure 4D).

With HSI, spectral data from each pixel were retained. Figure 5A shows the HIS of OP complexes. The spectra from OP complexes were randomly selected to develop a spectral library that represents the average spectrum of OP-complexed conjugates, and their individual spectrum is plotted in Figure 5B. Figure 5C shows the HIS of A549 cells without OP as a control. Using the spectral angle mapping (SAM) method, with the collected OP complex spectral library, no matching signal that represented the OP complex was mapped (Figure 5D). After incubation with OP complexes and a washing step, a significant number of OP complexes were visible on the cells (Figure 5E). Qualified signals representing OP complexes were located with the SAM method and quantified (Figure 5F).

CONCLUSIONS

A multifunctional nanocarrier system that can more efficiently deliver chemotherapeutic drugs and facilitate cancer tissue imaging while ameliorating the hypoxic tumor microenviron-

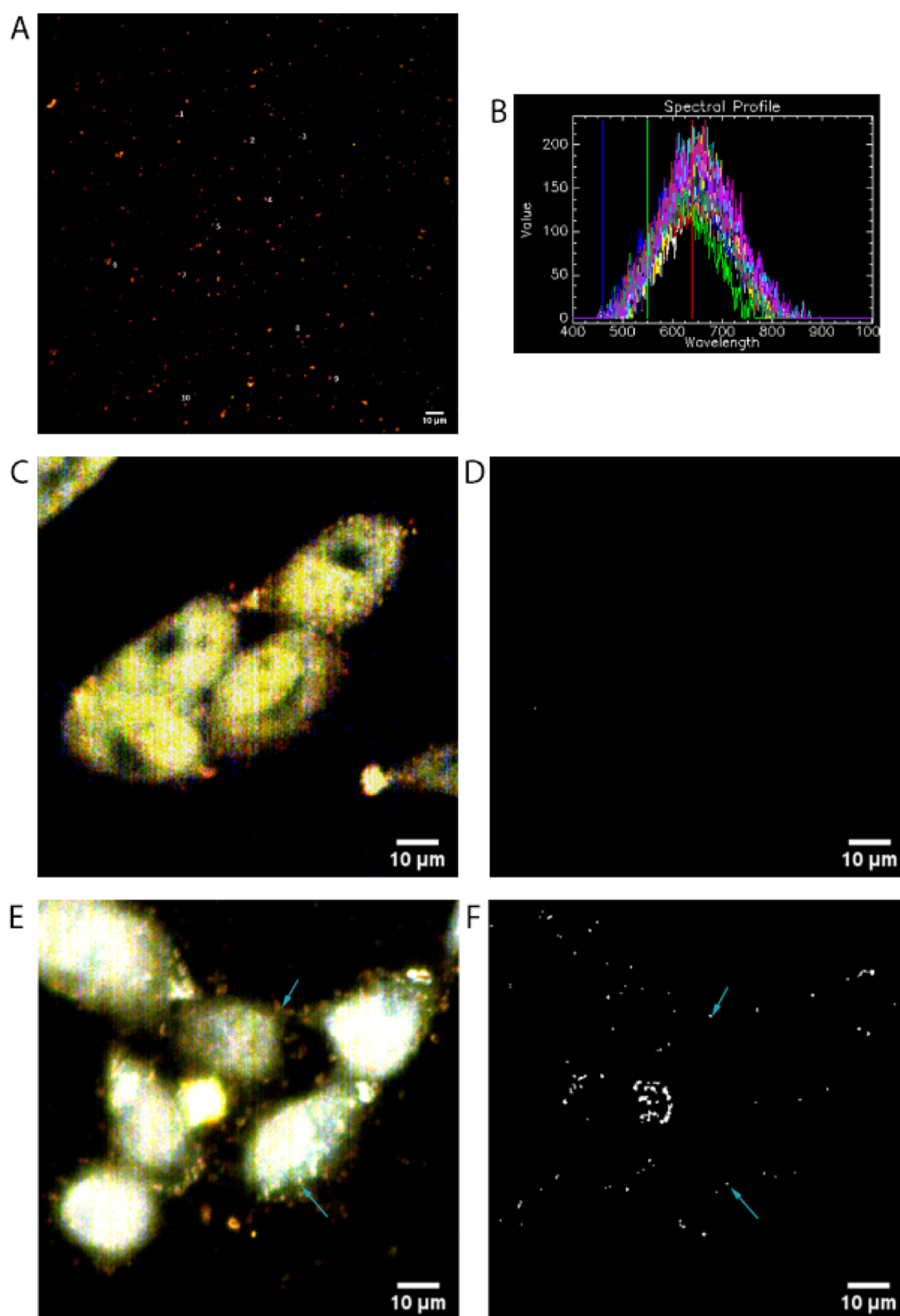


Figure 5. Darkfield microscopy hyperspectral imaging (HSI) of OPs and cells. (A) HSI image of OPs. (B) Spectral library of OPs taken in (A). (C) HSI of A549 cells only. (D) SAM of any signal that represents OPs in (C). (E) HSI of A549 cells incubated with the OP complex. (F) SAM of signals represents OPs in (E).

ment was constructed utilizing a functionalized OP complex conjugated with the targeting ligand and loaded with a drug, doxorubicin. Our results showed that the OPs can be fabricated in nano or micrometer sized ranges and doxorubicin could be successfully loaded onto the OPs due to an electrostatic interaction between the positively charged amine groups on doxorubicin and negatively charged carboxyl groups on the CMC. Anti-EGFR antibody was conjugated onto the

surface of OPs for specific targeting of EGFR expressing lung cancer cells to release doxorubicin in an acidic tumor microenvironment. Further, we show that drugs such as doxorubicin delivered through our OP complexes can significantly increase its efficacy against cancer cell proliferation. With DFM–HSI and further processing with SAM, we further demonstrate specific targeting of cancer cells and delivery of doxorubicin.

In conclusion, we have constructed a multifunctional nanocarrier system that can be loaded with chemotherapeutic drugs for targeted delivery to increase drug efficacy. The nanocarrier system is composed of the FDA approved CMC shell and oxygen core that can also be used to mitigate hypoxia. The developed approach constitutes a versatile theragnostic platform for the assessment of targeting efficacy and therapeutic efficacy of drugs for cancer and other diseases.

■ ASSOCIATED CONTENT

SI Supporting Information

The Supporting Information is available free of charge at <https://pubs.acs.org/doi/10.1021/acsomega.2c04953>.

Chemical structure of CMC chain, CMC OPs loaded with other chemicals, and image processing methodology (PDF)

■ AUTHOR INFORMATION

Corresponding Author

Joseph Irudayaraj – Department of Bioengineering, College of Engineering, University of Illinois Urbana-Champaign, Urbana, Illinois 61801, United States; Biomedical Research Center, Mills Breast Cancer Institute, Carle Foundation Hospital, Urbana, Illinois 61801, United States; Department of Comparative Biosciences, College of Veterinary Medicine and Cancer Center at Illinois; Carl R. Woese Institute for Genomic Biology; Beckman Institute; Micro and Nanotechnology Laboratory, University of Illinois Urbana-Champaign, Urbana, Illinois 61801, United States; orcid.org/0000-0002-0630-1520; Email: jirudaya@illinois.edu

Authors

Yi Wen – Department of Bioengineering, College of Engineering, University of Illinois Urbana-Champaign, Urbana, Illinois 61801, United States; Biomedical Research Center, Mills Breast Cancer Institute, Carle Foundation Hospital, Urbana, Illinois 61801, United States; Department of Comparative Biosciences, College of Veterinary Medicine, University of Illinois Urbana-Champaign, Urbana, Illinois 61801, United States

Wenjie Liu – Department of Bioengineering, College of Engineering, University of Illinois Urbana-Champaign, Urbana, Illinois 61801, United States; Biomedical Research Center, Mills Breast Cancer Institute, Carle Foundation Hospital, Urbana, Illinois 61801, United States

Benjamin David – Department of Bioengineering, College of Engineering, University of Illinois Urbana-Champaign, Urbana, Illinois 61801, United States

Wen Ren – Department of Bioengineering, College of Engineering, University of Illinois Urbana-Champaign, Urbana, Illinois 61801, United States; Biomedical Research Center, Mills Breast Cancer Institute, Carle Foundation Hospital, Urbana, Illinois 61801, United States

Complete contact information is available at: <https://pubs.acs.org/doi/10.1021/acsomega.2c04953>

Notes

The authors declare no competing financial interest.

■ ACKNOWLEDGMENTS

Y.W. and J.I. acknowledge the support from IETP Toxicology Scholar Award from UIUC.

■ REFERENCES

- (1) American Cancer Society. Facts & Figures 2021: Atlanta. 2021, <https://www.cancer.org/content/dam/cancer-org/research/cancer-facts-and-statistics/annual-cancer-facts-and-figures/2021/cancer-facts-and-figures-2021.pdf> (accessed 10 Jan, 2021).
- (2) Inamura, K. Lung cancer: understanding its molecular pathology and the 2015 WHO classification. *Front. Oncol.* **2017**, *7*, 193.
- (3) Ohsaki, Y. O.; Tanno, S. A.; Fujita, Y.; Toyoshima, E.; Fujiuchi, S.; Nishigaki, Y.; Ishida, S.; Nagase, A.; Miyokawa, N.; Hirata, S.; Kikuchi, K. Epidermal growth factor receptor expression correlates with poor prognosis in non-small cell lung cancer patients with p53 overexpression. *Oncol. Rep.* **2000**, *7*, 603–610.
- (4) Inamura, K.; Ninomiya, H.; Ishikawa, Y.; Matsubara, O. Is the Epidermal Growth Factor Receptor Status in Lung Cancers Reflected in Clinicopathologic Features? *Pathol. Lab. Med.* **2010**, *134*, 66–72.
- (5) Lee, C. K.; Brown, C.; Gralla, R. J.; Hirsh, V.; Thongprasert, S.; Tsai, C. M.; Tan, E. H.; Ho, J. C.; Chu, D. T.; Zatar, A.; Osorio Sanchez, J. A.; Vu, V. V.; Au, J. S. K.; Inoue, A.; Lee, S. M.; GebSKI, V.; Yang, J. C.-H. Impact of EGFR inhibitor in non-small cell lung cancer on progression-free and overall survival: a meta-analysis. *J. Natl. Cancer Inst.* **2013**, *105*, 595–605.
- (6) Nurgali, K.; Jagoe, R. T.; Abalo, R. Editorial: Adverse Effects of Cancer Chemotherapy: Anything New to Improve Tolerance and Reduce Sequelae? *Front. Pharmacol.* **2018**, *9*, 245.
- (7) Stewart, D. J.; Benjamin, R. S.; Luna, M.; Feun, L.; Caprioli, R.; Seifert, W.; Loo, T. L. Human tissue distribution of platinum after cis-diamminedichloroplatinum. *Cancer Chemother. Pharmacol.* **1982**, *10*, 51.
- (8) Johnson-Arbor, K.; Patel, H.; Dubey, R. *Doxorubicin*; StatPearls Publishing, 2017.
- (9) Karukstis, K. K.; Thompson, E. H.; Whiles, J. A.; Rosenfeld, R. J. Deciphering the fluorescence signature of daunomycin and doxorubicin. *Biophys. Chem.* **1998**, *73*, 249–263.
- (10) Motlagh, N. S.; Parvin, P.; Ghasemi, F.; Atyabi, F. Fluorescence properties of several chemotherapy drugs: doxorubicin, paclitaxel and bleomycin. *Biomed. Opt. Express* **2016**, *7*, 2400–2406.
- (11) Hervault, A.; Dunn, A. E.; Lim, M.; Boyer, C.; Mott, D.; Maenosono, S.; Thanh, N. T. Doxorubicin loaded dual pH- and thermo-responsive magnetic nanocarrier for combined magnetic hyperthermia and targeted controlled drug delivery applications. *Nanoscale* **2016**, *8*, 12152–12161.
- (12) Bhandari, P.; Novikova, G.; Goergen, C. J.; Irudayaraj, J. Ultrasound beam steering of oxygen nanobubbles for enhanced bladder cancer therapy. *Sci. Rep.* **2018**, *8*, 3112.
- (13) Wang, Y.; Newell, B. B.; Irudayaraj, J. Folic acid protected silver nanocarriers for targeted drug delivery. *J. Biomed. Nanotechnol.* **2012**, *8*, 751–759.
- (14) Meng, H.; Zou, Y.; Zhong, P.; Meng, F.; Zhang, J.; Cheng, R.; Zhong, Z. A Smart Nano-Prodrug Platform with Reactive Drug Loading, Superb Stability, and Fast Responsive Drug Release for Targeted Cancer Therapy. *Macromol. Biosci.* **2017**, *17*, 1600518.
- (15) Sirsi, S. R.; Borden, M. A. State-of-the-art materials for ultrasound-triggered drug delivery. *Adv. Drug Delivery Rev.* **2014**, *72*, 3–14.
- (16) Ding, C.; Li, Z. A review of drug release mechanisms from nanocarrier systems. *Mater. Sci. Eng., C* **2017**, *76*, 1440–1453.
- (17) Kim, C. K.; Ghosh, P.; Rotello, V. M. Multimodal drug delivery using gold nanoparticles. *Nanoscale* **2009**, *1*, 61–67.
- (18) Pontes, J. F.; Grenha, A. Multifunctional nanocarriers for lung drug delivery. *Nanomater* **2020**, *10*, 183.
- (19) Chen, J.; Irudayaraj, J. Fluorescence lifetime cross correlation spectroscopy resolves EGFR and antagonist interaction in live cells. *Anal. Chem.* **2010**, *82*, 6415–6421.

- (20) Wang, C.; Chen, J.; Talavage, T.; Irudayaraj, J. Gold nanorod/Fe₃O₄ nanoparticle “nano-pearl-necklaces” for simultaneous targeting, dual-mode imaging, and photothermal ablation of cancer cells. *Angew. Chem.* **2009**, *121*, 2797–2801.
- (21) Dhani, N.; Fyles, A.; Hedley, D.; Milosevic, M. The clinical significance of hypoxia in human cancers. *Semin. Nucl. Med.* **2015**, *45*, 110–121.
- (22) Brahim-Horn, M. C.; Chiche, J.; Pouysségur, J. Hypoxia and cancer. *J. Mol. Med.* **2007**, *85*, 1301–1307.
- (23) Bhandari, P. N.; Cui, Y.; Elzey, B. D.; Goergen, C. J.; Long, C. M.; Irudayaraj, J. Oxygen nanobubbles revert hypoxia by methylation programming. *Sci. Rep.* **2017**, *7*, 9268.
- (24) Bhandari, P.; Wang, X.; Irudayaraj, J. Oxygen nanobubble tracking by light scattering in single cells and tissues. *ACS Nano* **2017**, *11*, 2682–2688.
- (25) Badireddy, A. R.; Wiesner, M. R.; Liu, J. Detection, characterization, and abundance of engineered nanoparticles in complex waters by hyperspectral imagery with enhanced darkfield microscopy. *Environ. Sci. Technol.* **2012**, *46*, 10081–10088.
- (26) Patskovsky, S.; Bergeron, E.; Meunier, M. Hyperspectral darkfield microscopy of PEGylated gold nanoparticles targeting CD44-expressing cancer cells. *J. Biophot.* **2015**, *8*, 162–167.
- (27) Lee, K.; Cui, Y.; Lee, L. P.; Irudayaraj, J. Quantitative imaging of single mRNA splice variants in living cells. *Nat. Nanotechnol.* **2014**, *9*, 474.
- (28) Cui, Y.; Wang, X.; Ren, W.; Liu, J.; Irudayaraj, J. Optical clearing delivers ultrasensitive hyperspectral dark-field imaging for single-cell evaluation. *ACS Nano* **2016**, *10*, 3132–3143.
- (29) Cho, S.-H.; Kim, J. Y.; Chun, J. H.; Kim, J. D. Ultrasonic formation of nanobubbles and their zeta-potentials in aqueous electrolyte and surfactant solutions. *Colloids Surf., A* **2005**, *269*, 28–34.
- (30) Bethune, G.; Bethune, D.; Ridgway, N.; Xu, Z. Epidermal growth factor receptor (EGFR) in lung cancer: an overview and update. *J. Thorac. Dis.* **2010**, *2*, 48.
- (31) Liu, W.; Biton, E.; Pathania, A.; Matityahu, A.; Irudayaraj, J.; Onn, I. Monomeric cohesin state revealed by live-cell single-molecule spectroscopy. *EMBO Rep.* **2020**, *21*, No. e48211.
- (32) Zheng, L.; Wen, Y.; Ren, W.; Duan, H.; Lin, J.; Irudayaraj, J. Hyperspectral dark-field microscopy for pathogen detection based on spectral angle mapping. *Sens. Actuators, B* **2022**, *367*, 132042.
- (33) Hulst, H. C.; van de Hulst, H. C. *Light Scattering by Small Particles*; Courier Corporation, 1981.
- (34) Hoshyar, N.; Gray, S.; Han, H.; Bao, G. The effect of nanoparticle size on in vivo pharmacokinetics and cellular interaction. *Nanomedicine* **2016**, *11*, 673–692.
- (35) Bhandari, P.; Irudayaraj, O.; Irudayaraj, J. Hypoxia reprogramming oxygen nanobubbles sensitize human glioblastoma cells to temozolomide via methylation alterations. *J. Bionanoscience* **2017**, *11*, 337–345.
- (36) Jin, H.; Lovell, J. F.; Chen, J.; Ng, K.; Cao, W.; Ding, L.; Zhang, Z.; Zheng, G. Investigating the specific uptake of EGF-conjugated nanoparticles in lung cancer cells using fluorescence imaging. *Cancer Nanotechnol.* **2010**, *1*, 71–78.
- (37) Kurai, J.; Chikumi, H.; Hashimoto, K.; Yamaguchi, K.; Yamasaki, A.; Sako, T.; Touge, H.; Makino, H.; Takata, M.; Miyata, M.; Nakamoto, M.; Burioka, N.; Shimizu, E. Antibody-dependent cellular cytotoxicity mediated by cetuximab against lung cancer cell lines. *Clin. Cancer Res.* **2007**, *13*, 1552–1561.
- (38) Perrin, D.; Dempsey, B.; Serjeant, E. P. *pKa prediction for organic acids and bases*; Chapman and Hall: London, 1981; p 1.
- (39) National Center for Biotechnology Information. PubChem Compound Summary for CID 31703, Doxorubicin, <https://pubchem.ncbi.nlm.nih.gov/compound/Doxorubicin> (Accessed 29 Sept, 2022).